Analytical Methods

RSC Publishing

TECHNICAL NOTE

View Article Online
View Journal | View Issue

Cite this: *Anal. Methods*, 2013, **5**, 4268

Vapor discrimination by dual-laser reflectance sensing of a single functionalized nanoparticle film†

Kee Scholten,‡[ab] Karthik Reddy,‡[acd] Xudong Fan[ac] and Edward T. Zellers*[aef]

Received 10th June 2013
Accepted 4th July 2013

DOI: 10.1039/c3ay40952j

www.rsc.org/methods

Sorption-induced changes in the localized surface-plasmon resonance (LSPR) of an *n*-octanethiolate-monolayer-protected gold nanoparticle film on a Si chip are exploited to differentiate two volatile organic compounds (VOC) with a single sensor. Probing the film with 488 nm and 785 nm lasers gave reflectance sensitivity ratios at the two wavelengths of 0.68 and 0.80 for toluene and *n*-heptane, respectively, permitting their discrimination. Swelling-induced increases in inter-particle distance appear to predominate over changes in the refractive index of the inter-particle matrix in the sensor responses. The corresponding ratios of sensitivities with a reference film of polydimethylsiloxane did not differ for the two vapors. Approaches for extending the capability for VOC discrimination by use of arrays of such LSPR sensors are discussed, along with the advantages of employing this simple platform in compact, field-deployable environmental VOC monitoring systems.

Introduction

Optical sensing of biological and chemical analytes by means of devices and/or materials with engineered nanoscale features has been studied extensively.[1,2] In regard to the measurement of airborne volatile organic compounds (VOC), sensing on the basis of absorbance, reflectance, or Raman scattering has been implemented using metallic,[3,4] organometallic,[5–7] and polymeric nanoparticles,[8] as well as photonic crystals[9] and lamellar gratings or reflectors.[10] The utility of localized surface plasmon resonances (LSPR) in liquid-phase (bio)chemical analyses has been recognized for some time,[2,11,12] but has only recently been applied to the detection of gases[13] and VOCs.[3,5–7,10,14]

By use of unmodified grating structures[10] or surface-patterned metal nano-islands with either polymer overlay films[3] or thiolate-monolayer functionalization,[14] it has been shown that LSPR spectral shifts differ among VOCs on the basis of differential changes in the refractive index (RI) of the interstitial matrix accompanying vapor sorption. For example, Potyrailo *et al.* measured visible reflectance changes due to vapor exposure in unmodified naturally occurring lamellar gratings (*i.e.*, Morpho butterfly wings), and extracted responses at four selected wavelengths to discriminate among high concentrations of methanol, ethanol and water vapor, and among the three isomers of dichloroethylene.[10] Karakouz *et al.* reported on polymer-coated gold nano-islands, showing differences in the magnitude of LSPR maxima (λ_{max}) shifts with polar and non-polar polymers according to vapor affinity,[3] and Chen *et al.* used thiolate-monolayer functionalized gold nano-islands to detect terpene vapors.[14]

Others have used films of discrete thiolate-monolayer-protected gold nanoparticles (MPN) as plasmonic interface materials,[5–7] complementing the well-documented use of MPNs as vapor-sorptive layers on chemiresistors (CR) and thickness shear mode resonators (TSMR).[15–21] For example, Lu *et al.* used monolayer films of various metal MPNs to detect several VOCs by measuring changes in total absorbance or shifts in λ_{max}.[5] In their subsequent study of functionalized Ag, Au, and Au core–shell MPN films, they showed that sorption-induced changes in absorbance in the vicinity of λ_{max} among several films could be used for VOC discrimination.[6] More recently, Dalfovo *et al.* attributed observed differences in the shifts of the LSPR λ_{max} of tetraoctylammonium bromide (TOAB) functionalized MPN films upon exposure to saturated headspace concentrations of toluene and ethanol to differences in film swelling/shrinkage and RI changes by the two VOCs.[7]

The results of these studies suggest that discriminating among VOCs by use of a single MPN-coated optical sensor should be possible, and that it could be achieved by probing the MPN film at as few as two wavelengths. This would obviate the need for a spectrometric detector, as used in all previous studies

[a]*Center for Wireless Integrated MicroSensing and Systems, University of Michigan, Ann Arbor, MI 48109-2121, USA. E-mail: ezellers@umich.edu*

[b]*Applied Physics Program, University of Michigan, Ann Arbor, MI 48109-1040, USA*

[c]*Department of Biomedical Engineering, University of Michigan, Ann Arbor, MI 48109-2110, USA*

[d]*Department of Electrical Engineering and Computer Science, University of Michigan, Ann Arbor, MI 48109-2121, USA*

[e]*Department of Environmental Health Sciences, University of Michigan, Ann Arbor, MI 48109-2029, USA*

[f]*Department of Chemistry, University of Michigan, Ann Arbor, MI 48109-1055, USA*

† Electronic supplementary information (ESI) available: Discussion and accompanying spectra of a C8-MPN film exhibiting persistent changes to the LSPR band following exposure to saturated headspace concentrations of toluene vapor. See DOI: 10.1039/c3ay40952j

‡ These authors contributed equally.

of this nature, and would facilitate configuring a small, portable system suitable for field deployment. Here, we describe such a device and present preliminary results demonstrating such capabilities. The visible absorbance spectra of an *n*-octanethiolate (C8) MPN film before, during, and after exposure to vapors of toluene and *n*-heptane are presented first to characterize the nature of the spectral changes and to confirm reversibility of the vapor-film interaction. Then laser reflectance measurements at two discrete wavelengths are presented, demonstrating the discrimination of the two VOCs on the basis of the ratios of responses at these wavelengths. The relative importance of changes in the film RI and film swelling to the differential responses at different wavelengths are discussed as well as methods by which diversity of responses might be further enhanced.

Materials and methods

C8-MPNs were synthesized according to the method of Rowe *et al.*,[15] with an average Au core diameter of 4.3 ± 0.9 nm. Polydimethylsiloxane (PDMS, Fluka, St. Louis, MO) was used as a reference material. Toluene and *n*-heptane (99%, Sigma Aldrich, St. Louis, MO) were used as received. The values of RI, density, and vapor pressure for these two test vapors are as follows:[22] toluene, 1.496, 0.867 g mL^{-1}, and 2.91 kPa (20 °C); *n*-heptane, 1.387, 0.684 g mL^{-1}, and 4.63 kPa (20 °C). The RI of the octanethiol monolayer was assumed to be the RI of 1-octanethiol, 1.45.[22]

A glass slide was diced manually to dimensions of 45 × 10 mm to fit inside a 3 mL plastic cuvette, and 8 × 8 mm chips of ⟨100⟩ Si were diced from a 4-inch wafer with a dicing saw. Substrates were cleaned sequentially in acetone and isopropanol while immersed in an ultrasonic bath, blown dry, and then exposed to vapors of hexamethyldisilazane (HMDS) to promote adhesion of the C8-MPN or PDMS films. Films were deposited from dilute (5 mg mL^{-1}) solutions of C8-MPNs in toluene by spray coating with an airbrush ~30 cm from the substrate using air at approximately 140 kPa as the propellant. Thickness and uniformity were assessed by optical microscopy and laser interferometry (LEXT, Olympus, Tokyo, Japan). PDMS was spin-coated at 7600 rpm onto a Si chip from a 5 mg mL^{-1} toluene solution. The thickness was estimated to be 1–1.2 μm. (Note: MPN films could not be cast effectively by spin coating.)

The MPN-coated glass slide was placed vertically in the plastic cuvette and the visible absorbance spectrum was measured (DU800 UV-Vis spectrophotometer Beckman Coulter, Brea, CA). The effects of vapor exposure were assessed initially by placing ~1.5 μL of liquid VOC in the lid of the cuvette and quickly capping it so that the film was exposed to a high concentration of the vapor. The spectrum was collected and then the lid was removed to allow the vapor to dissipate for 20 min prior to collecting another spectrum. A blank spectrum was collected with an uncoated slide similarly in a sealed cuvette. Separate exposures to toluene and *n*-heptane were performed in duplicate. Replicate spectra were superimposable.

A microfluidic enclosure, 1 mm deep and 0.85 mm wide, was formed from three glass slides using UV-curable glue and sealed to the underlying MPN-coated Si chip with adhesive. An identical microfluidic enclosure was affixed to the PDMS coated Si chip. The ensemble was mounted to an adjustable metal stage with double sided tape. The upstream end of a 5 m long, fused silica capillary (250 μm i.d., Restek, Bellefonte, PA) was attached to the injection port of a benchscale gas chromatograph (3800, Varian, Inc., Palo Alto, CA) and the downstream end was inserted into the inlet of the microfluidic enclosure and sealed. Helium was used as the carrier gas at 8 mL min^{-1}.

Fig. 1 depicts the measurement configuration. The coated Si chip was illuminated sequentially by a 785 nm tunable diode laser and a 488 nm diode pumped solid state laser, and the intensity of the reflected beam was measured by a CMOS detector (Thor Labs DCC1240M, Newton, NJ) with an acquisition time of 1–4 μs and a save rate of 20 frames per second. The 785 nm laser had a 0.8 mW output while the 488 nm laser had a 10.8 mW output filtered down to 0.15 mW. These wavelengths were selected because they bracket λ_{max} for the C8-MPN film. A 30° angle of incidence was found to give the largest responses at both wavelengths, and was fixed for all experiments. Reflected intensity at each wavelength was recorded during separate dynamic exposures to toluene and *n*-heptane over a five-fold range of concentration by injecting 40, 80, 150 and 200 μL (corresponding to 4.3–22 μg of toluene and 8.6–43 μg of *n*-heptane) of headspace above the liquid solvents by gas-tight syringe into the GC injection port at 250 °C. Injected mass was calculated assuming saturation of the headspace at 20 °C. Due to higher sensitivity of the PDMS film, calibrations were performed with a 10 000 : 1 injection split. Measurements were taken at each wavelength sequentially, with 4–5 replicates collected at each exposure level.

Data were analyzed using Origin software (v. 8.5.1, OriginLab, Northampton, MA). A 20-point fast Fourier transform algorithm was used to smooth the data. Sensor response was defined as the integrated peak area (detector counts × seconds) averaged across all replicates. A set of calibration curves plotting sensor response as a function of injection mass was generated, and the sensitivity was defined as the slope of the resulting line as determined by least-squares regression with forced zero y-intercept.

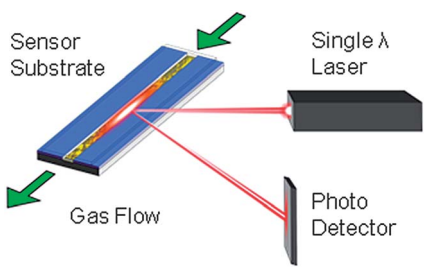

Fig. 1 Illustration of the apparatus used for laser reflectance measurements of C8-MPN and PDMS films during calibrations with toluene and *n*-heptane. Discrete injections of different quantities of each vapor were made *via* a heated GC injection port and were routed through the microfluidic cell *via* de-activated capillary at 8 mL min^{-1} (carrier gas was He).

Results and discussion

MPN film characterization

Spray-coated C8-MPN films appeared homogeneous by visual inspection but microscopically were shown to comprise dense, multilayer coated sections surrounded by areas of uncoated substrate (Fig. 2a). Laser interferometry at five locations (each 130 × 130 μm) of one representative film indicated an average film thickness (coated regions) of 260 nm with a standard deviation (SD) of 90 nm. The visible absorbance spectrum in Fig. 2b shows a broad LSPR peak with λ_{max} at 536.0 nm. The spectrum of C8 MPNs of similar Au-core size in toluene solution was reported to give a λ_{max} of 517 nm.[15] The red shift in λ_{max} and broadness of the absorbance of the airbrushed film reflects the expected increase in optical coupling between the Au cores associated with the smaller inter-particle spacing.[23]

Responses to vapors: absorbance spectra

Blue shifts in λ_{max} to 530.6 nm and 533.4 nm were observed during separate, static exposures of a C8-MPN film to near-saturated concentrations of toluene and *n*-heptane vapors, respectively. In general, shifts in λ_{max} can arise from two separate phenomena: an increase in the inter-particle distance due to film swelling and a change in the RI of the medium surrounding the nanoparticles.[22] The former will cause a blue shift in λ_{max} and the effect of the latter will depend on the RI difference between the inter-particle matrix of the MPN film and the sorbed vapor; if the RI of the sorbed vapor is higher than that of the organic matrix, then a red shift is expected, and if it is lower, then a blue shift is expected. The blue shift in λ_{max} for *n*-heptane is consistent with its RI being lower than that of the C8 monolayer (bulk value) and its ability to swell the film. The blue shift in λ_{max} for toluene, the RI of which is slightly higher than that of C8, indicates that swelling dominates the optical response. A similar result (and explanation) was reported by Dalfovo *et al.* for 4.4 nm TOAB–MPN films exposed to saturated toluene vapor,[7] in spite of the RI for TOAB (*i.e.*, $n = 1.42$) being lower than that of toluene. The larger shift in λ_{max} for toluene, compared to *n*-heptane, observed here can be attributable to its larger partition coefficient and swelling efficiency (see below).[20] Although λ_{max} returned to its pre-exposure value upon subsequent venting of the cuvette with room air in the experiments above, we have also observed that extended exposure to saturated concentrations of toluene led to a persistent loss of the LSPR absorbance, which was recovered only after re-casting the same film from liquid toluene (see ESI†).

In addition to shifts in λ_{max}, absorbance changes within selected spectral regions occurred that differed between the two VOCs: for all $\lambda > \lambda_{max}$ exposure to either VOC reduced the magnitude of the absorbance, while for all $\lambda < \lambda_{max}$ toluene increased the absorbance and *n*-heptane decreased the absorbance. As shown in the inset of Fig. 2b, absorbance at λ_{max} increased during toluene exposure and decreased during *n*-heptane exposure. This analyte-dependent difference in sorption-induced changes in spectral features implies that selective sensing would be possible by probing the MPN film at multiple discrete wavelengths.

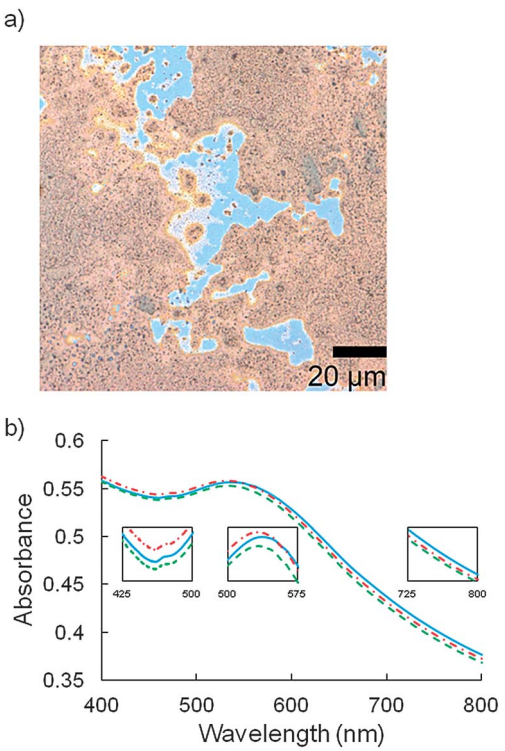

Fig. 2 (a) Optical micrograph (1000×) of a C8-MPN film on a Si substrate; (b) visible absorbance spectrum of a C8-MPN coated glass slide prior to exposure (solid blue line), during static exposure to *n*-heptane (dashed green line), and during static exposure to toluene (dashed-dotted red line). Insets show enlargements of selected spectral regions. Absorbance was measured with reference to a blank glass slide.

Responses to vapors: reflectance measurements

Toward that end, a C8-MPN film was coated on a clean Si substrate, enclosed in a glass microfluidic cell, and exposed to discrete injections of each VOC over a range of vapor concentrations while laser reflectance measurements were collected at 488 and 785 nm. At both wavelengths and for both analytes, the reflected intensity decreased with increasing injected analyte mass. Fig. 3a and b show calibration curves for both vapors, which fit linear models well ($r^2 > 0.97$, standard errors of the slopes < 6%) (note: changes in reflected intensity can be attributed to a combination of absorbance, reflectance, and scattering). Calculated sensitivities (peak area per μg of injected vapor) at 785 nm are 9.5×10^{-3} and 3.2×10^{-3} for toluene and *n*-heptane, respectively, and at 488 nm are 14×10^{-3} and 4.0×10^{-3}, respectively. The representative response profiles shown in the inset of Fig. 3a document the reversibility and repeatability of the responses.

The relative magnitudes of the sensitivities can be assessed in light of a previous study by Steinecker *et al.* of vapor uptake by films C8-MPNs with ~4.3 nm Au-core diameters on CR and TSMR sensors.[24] Partition coefficients (K_{voc}) and fractional film swelling efficiencies (Ψ_{voc}) for both toluene and *n*-heptane in C8-MPN films were derived from their data. Values of $K_{tol} = 1000$ and $K_{hep} = 410$ were reported along with values of $\Psi_{tol} = 0.32$ and $\Psi_{hep} = 0.23$. From these values we calculate a net swelling ratio of 3.4 (*i.e.*, $K_{tol}/K_{hep} \times \Psi_{tol}/\Psi_{hep}$).

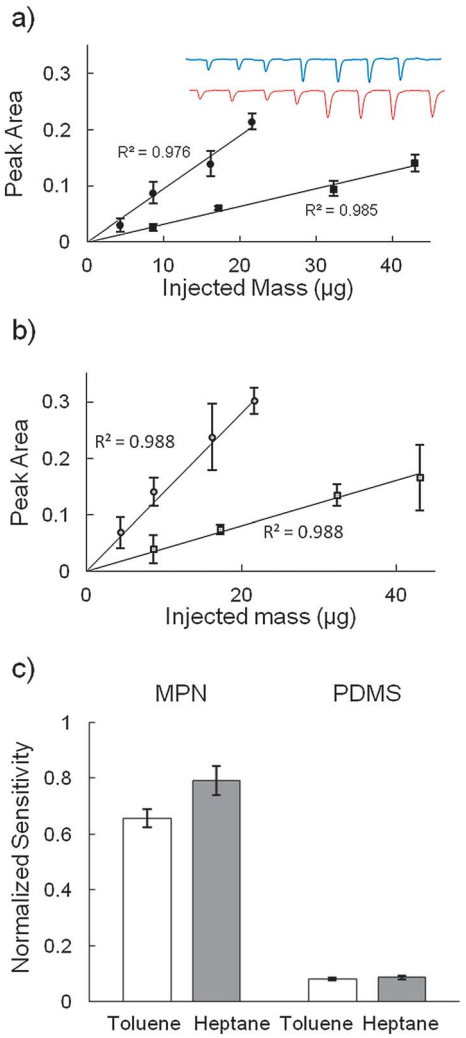

Fig. 3 (a) 785 nm and (b) 488 nm laser reflectance calibration curves for vapors of toluene (circles) and *n*-heptane (squares) from a single C8-MPN coated Si device. Peak area is plotted *versus* the injected mass of vapor. Error bars designate ±1 standard deviation ($n = 4$ or 5 injections) and are attributed to imprecision in injected masses rather than inherent variability in responses. R^2 values are from linear regression with a forced-zero intercept. Inset in (a) shows a representative series of response profiles (peaks) for *n*-heptane (upper trace) and toluene (lower trace) at 785 nm. Bar charts in (c) show sensitivities to each vapor at 785 nm for the C8-MPN and PDMS coated devices (as indicated) normalized to the sensitivity at 488 nm. Error bars indicate ±one standard error of the slope.

Since the dynamic exposures in this study were conducted under the same conditions for both VOCs, producing similar peak widths, the vapor concentrations should be similar for a given injected mass. The toluene : *n*-heptane sensitivity ratios are 2.97 and 3.60 at 785 nm and 488 nm, respectively, which are remarkably close to the swelling ratio of 3.4. This suggests that the relative responses are dictated *primarily* by the relative volumetric changes of the film. That the sensitivity ratio at 488 nm is somewhat larger, and the sensitivity ratio at 785 nm is somewhat smaller, than the calculated swelling ratio is qualitatively consistent with the differences in absorbance between toluene and *n*-heptane noted above for the spectral regions flanking λ_{max}. Such wavelength-dependent differences reflect the (secondary) contributions of the RI changes to the optical responses.

In the reflectance measurements, the toluene sensitivity was higher at 488 nm than at 785 nm, which is consistent with the spectrophotometric data that showed an increase in absorbance at $\lambda < \lambda_{max}$. But, whereas the reflectance measurements showed *decreases in reflected intensity* at the longer wavelength for toluene and at both wavelengths for *n*-heptane, the spectrophotometric measurements showed *decreases in absorbance* for these exposures. This discordance can be ascribed to differences in these two optical configurations; specifically to an increase in the extent of scattered and reflected light from the air–film and substrate–film interfaces in the reflectance measurements.[25,26]

Limits of detection (LOD) were calculated as 3σ/(sensitivity) where σ was the standard deviation of the baseline signal and the sensitivity was re-calculated using peak height instead of area. LODs at 785 nm are 0.20 and 0.49 μg for toluene and heptane, respectively, and at 488 nm are 1.1 and 3.3 μg, respectively. The LODs are higher at 488 nm, despite the higher sensitivities at this wavelength, because of the increased noise from the 488 nm laser; the baseline noise at 785 nm was eight times lower than at 488 nm. No effort was made to optimize the set-up for sensitivity.

Measurements were also collected in the same manner with a reference Si substrate coated with PDMS. Since PDMS has no absorbance in the visible range, changes in reflected light intensity arise only from changes in the film thickness. This phenomenon is exploited in vapor sensors that are based on Fabry–Perot interferometry.[27] Responses were proportional to injected vapor mass and calibration curves were linear ($r^2 >$ 0.97, standard slope error < 5%). Since the PDMS exposures were performed with split injections from the GC and the PDMS film was ~4–5 times thicker than the MPN film, a direct comparison of sensitivities and LODs is not possible. However, it can be stated that the PDMS film showed much higher sensitivities than did the MPN film, with LODs in the sub-ng range for both VOCs, consistent with previous reports of similarly configured PDMS-coated optical sensors.[27]

The bar charts in Fig. 3c present the ratios of the sensitivities at the two wavelengths for toluene and *n*-heptane for both films, normalized to that at 488 nm, which gave the highest sensitivity in all cases. For the C8-MPN film the average (±SD) ratios are 0.68 ± 0.035 and 0.80 ± 0.053 for toluene and *n*-heptane. The corresponding ratios for the PDMS reference film are 0.082 ± 0.005 and 0.088 ± 0.006. The difference between the MPN ratios is statistically significant ($p < 0.05$), whereas the difference between the PDMS ratios is not ($p > 0.20$), confirming that vapor discrimination is a function of the optical properties of the MPN film.

Conclusions

We have shown that dual-wavelength optical reflectance sensing of a single MPN film exhibiting LSPR affords quantitative and qualitative information about airborne VOCs. In this proof-of-concept study, the discrimination of two non-polar VOCs on the basis of wavelength-specific differences in reflected light intensity was demonstrated with a simple platform comprising a single LSPR sensor enclosed in a microfluidic cell, two laser sources, and a photodetector. Unlike previous reports

of optical VOC detection with such materials, which employed spectrophotometric analyzers, the system described here could be readily miniaturized and incorporated into a compact, portable system suitable for wearable and/or distributed environmental VOC monitoring.

Reversible blue shifts in the LSPR λ_{max} were observed for high-concentration exposures to both toluene and *n*-heptane, despite their RI values flanking that of the C8 monolayers in the MPNs tested here. These results, coupled with estimates of swelling ratios derived from independent data, suggest that responses are determined primarily by increases in the average inter-particle distance of the MPNs accompanying sorption-induced film swelling, and secondarily by changes in the local RI. In contrast, LSPR sensing approaches that employ immobilized gold nano-islands are only sensitive to shifts in the local RI of the surrounding medium.[3,14]

The use of multiple, discrete, optical probes of individual plasmonic sensing films shown here is an example of what might be termed multi-variable (MV) sensing. Other examples have been reported by Potyrailo *et al.*[10,28] Creating an array of such MV sensors in which multiple films of MPNs with different core sizes, shapes, and/or monolayer structures are probed at *two or more* wavelengths shows promise for increasing the diversity of responses one can obtain from a VOC sensor array. This, in turn, should lead to improvements in performance over current single-transducer (ST) and multi-transducer (MT) arrays, which provide only a single response from each sensor in the array and, consequently, have only limited capabilities for VOC-mixture analysis.[29,30]

Although the sensitivity achieved with the C8-MPN sensing film here was quite low, enhanced sensitivity should be possible by use of high-quality-factor optical resonators, in which optical signals are amplified by photon recirculation.[31] A parallel effort in our laboratory on the development of microfabricated opto-fluidic ring resonators (μOFRR) as platforms for multi-wavelength sensing with MPN interface films has shown some promising results in preliminary testing.[32,33]

Acknowledgements

The authors express their heartfelt appreciation to Ms Lindsay Wright for MPN synthesis and other technical assistance. This work was supported by NSF Grant ECCS 1128157 and by the NIH Microfluidics in Biomedical Sciences Training Program Grant 2T32EB005582-06.

References

1 A. Shipway, E. Katz and I. Willner, *ChemPhysChem*, 2000, **1**, 18–52.
2 M. Stewart, C. Anderton, L. Thompson, J. Maria, S. Gray, J. Rogers and R. Nuzzo, *Chem. Rev.*, 2008, **108**, 494–521.
3 T. Karakouz, A. Vaskevich and I. Rubenstein, *J. Phys. Chem.*, 2008, **112**, 14530–14538.
4 M. K. Oo, C. F. Chang, Y. Sun and X. Fan, *Analyst*, 2011, **136**, 2811–2817.
5 C.-S. Cheng, Y.-Q. Chen and C.-J. Lu, *Talanta*, 2007, **73**, 358–365.
6 K.-J. Chen and C.-J. Lu, *Talanta*, 2010, **81**, 1670–1675.
7 M. Dalfovo, R. Salvarezza and F. Ibanez, *Anal. Chem.*, 2012, **84**, 4866–4892.
8 T. Endo, Y. Yanagida and T. Hatsuzawa, *Sens. Actuators, B*, 2007, **12**, 589–595.
9 T. L. Kelly, A. G. Sega and M. J. Sailor, *Nano Lett.*, 2011, **11**, 3169–3173.
10 R. Potyrailo, H. Ghiradella, A. Vertiatchikh, K. Dovidenko, J. Cournoyer and E. Olson, *Nat. Photonics*, 2007, **1**, 123–128.
11 N. Nath and A. Chilkoti, *Anal. Chem.*, 2002, **74**, 504–509.
12 A. Kabashin, P. Evans, S. Pastkovsky, W. Hendren, G. A. Wurtz, R. Atkinson, R. Pollard, V. A. Podolskiy and A. V. Zayats, *Nat. Mater.*, 2009, **8**, 867–871.
13 M. Nandasiri, P. H. Rogers, W. Jiang, T. Varga, S. V. N. T. Kuchibhatla, S. Thevuthasan and M. A. Carpenter, *Anal. Chem.*, 2012, **84**, 5025–5034.
14 B. Chen, C. Liu, M. Ota and K. Hayashi, *IEEE Sens. J.*, 2013, **13**, 1307–1314.
15 M. Rowe, K. Plass, K. Kim, Ç. Kurdak, E. T. Zellers and A. Matzger, *Chem. Mater.*, 2004, **18**, 3513–3517.
16 F. I. Bohrer, E. Covington, Ç. Kurdak and E. T. Zellers, *Anal. Chem.*, 2011, **83**, 3687–3695.
17 C.-L. Li, Y.-F. Chen, M.-H. Liu and C.-J. Lu, *Sens. Actuators, B*, 2012, **169**, 349–359.
18 J. Grate, D. Nelson and R. Skaggs, *Anal. Chem.*, 2003, **75**, 1868–1879.
19 N. Krasteva, I. Besnard, B. Guse, R. Bauer, K. Mullen, A. Yasuda and T. Vossmeyer, *Nano Lett.*, 2002, **2**, 551–555.
20 L. Wang, X. Shi, N. Kariuki, M. Schadt, M. G. Wang, Q. Rendeng, J. Choi, J. Luo, S. Lu and C.-J. Zhong, *J. Am. Chem. Soc.*, 2007, **129**, 2161–2170.
21 S. Kim, H. Chang and E. T. Zellers, *Anal. Chem.*, 2011, **83**, 7198–7206.
22 *CRC Handbook of Chemistry and Physics*, 93rd edn, Internet Version 2013, http://www.hbcpnetbase.com/.
23 A. Templeton, J. Pietron, R. Murray and P. Mulvaney, *J. Phys. Chem. B*, 2000, **104**, 564–570.
24 W. Steinecker, M. Rowe and E. T. Zellers, *Anal. Chem.*, 2007, **79**, 4977–4986.
25 G. Gauglitz, A. Brecht, G. Kraus and W. Nahm, *Sens. Actuators, B*, 1993, **11**, 21–27.
26 G. G. Daaboul, R. S. Vedula, S. An, C. A. Lopez, A. Reddington, E. Ozkumur and M. S. Ünlü, *Biosens. Bioelectron.*, 2011, **26**, 2221–2227.
27 K. Reddy, Y. Guo, J. Liu, W. Lee, M. Oo and X. Fan, *Sens. Actuators, B*, 2011, **159**, 60–65.
28 R. Potyrailo and W. Morris, *Anal. Chem.*, 2007, **79**, 45–51.
29 C. Jin and E. T. Zellers, *Anal. Chem.*, 2008, **80**, 227–236.
30 C. Jin and E. T. Zellers, *Anal. Chem.*, 2008, **80**, 7283–7293.
31 F. Vollmer and S. Arnold, *Nat. Methods*, 2008, **5**, 591–596.
32 K. Scholten, X. Fan and E. T. Zellers, *Appl. Phys. Lett.*, 2008, **99**, 141108.
33 K. Scholten, X. Fan and E. T. Zellers, *Tech. Digest Transducers'13*, Barcelona, Spain, June 16–20, 2013, pp. 850–853.

